Thermochimica Acta 507–508 (2010) 77–83

Contents lists available at ScienceDirect

Thermochimica Acta

journal homepage: www.elsevier.com/locate/tca

Comparison in thermal behaviors of homologues, derivatives and adducts of β-cyclodextrin

Lin Hong Zhu [a], Le Xin Song [a,b,*], Xue Qing Guo [b], Zheng Dang [b]

[a] CAS Key Laboratory of Soft Matter Chemistry, Department of Chemistry, University of Science and Technology of China, Hefei 230026, PR China
[b] Department of Polymer Science and Engineering, University of Science and Technology of China, Hefei 230026, PR China

ARTICLE INFO

Article history:
Received 18 March 2010
Received in revised form 28 April 2010
Accepted 30 April 2010
Available online 19 May 2010

Keywords:
Cyclodextrin
Homologue
Derivative
Adduct
Thermal behavior

ABSTRACT

The thermal behaviors of homologues, derivatives and adducts of β-cyclodextrin (β-CD) are compared based on thermogravimetry (TG) and gas chromatography coupled to time-of-flight mass spectrometry (GC–TOF-MS) analysis. Our results indicate that the number of glucose units and the introduced groups cause a considerable change in thermal decomposition mechanisms of these carbohydrates. Further, it is observed that the mass loss of the bicomponent aggregate formed by phenylarsonic acid (PAA) and β-CD is larger than that of each of the components at higher temperatures. Additionally, the decomposition of the adduct produces a series of arsenic compounds with high relative abundances, such as AsO^+, $As_2O_2^+$, $As_3O_4^+$ and $As_4O_6^+$, which is rather different from the decomposition behaviors of free PAA and the adduct of β-CD with sodium arsenite.

1. Introduction

α-, β- and γ-cyclodextrins (CDs) are three most common types of CDs composed of 6, 7 and 8 *D*-glucopyranose units, respectively, and shaped as truncated cones [1–3]. A great number of guest–CD complexes have been investigated in solution or in solid state, due to their various compositions, special structures and excellent properties that cover a wide range of applications such as food, perfumery, cosmetics, pharmaceutical and winery industries [4–7]. The change in thermal stability of guests due to the interaction between them and CDs is one of the most important reasons that CDs can be used so widely [8,9]. However, until now few data have been available to compare the difference of thermal degradation mechanisms of CDs, as well as to understand the negative consequences of thermal degradation fragments of them. This is one of our motivations for this article.

Although β-CD is very inexpensive, non-toxic and safe to use and dispose, the small cavity size and poor solubility in water limit its application [10,11]. This problem could be removed by introducing appropriate substituents at the hydroxyl moiety of β-CD [12–14]. Numerous derivatives of β-CD have been synthesized and applied in different research aspects [15–19]. Positive performance of "structural modification" effects has received considerable attention [20,21]. On the contrary, the negative contribution of the "structural modification" is little mentioned in the literature in spite of its importance in evaluating the practical application of modified β-CDs. Here, we attempt to recognize a significant problem: how does the introduction of substituent groups affect the degradation mechanism of parent β-CD?

There are many reports on the thermal properties of inclusion complexes of β-CD with organic guests [22,23]. The question needs to be faced: whether the complexes obtained in different methods are pure compounds? Of course, the purification of them is a difficult issue because there is a high similarity between β-CD and its complexes in physical and chemical properties. Also, there is the possible influence of equilibrium of host–guest complexation in solution. It is well known that arsenic compounds have two faces: high toxicity and wide usage. Recently, it was found that a simple mixing process between β-CD and a compound such as sodium arsenite ($NaAsO_2$, SA) in water can realize the goal of seriously changing the thermal behavior of the compound [24]. This result encourages us to pursue the study to other arsenic compounds such as phenylarsonic acid (PAA), an important component of industrial wastes, in order to examine the difference of effect of adduct interaction on thermal degradation performances of inorganic and organic arsenic compounds.

According to these aspects, initially, we compare the thermal characteristics of α-, β- and γ-CD on the basis of thermogravimetry (TG) especially gas chromatography coupled to time-of-flight mass spectrometry (GC–TOF-MS) analyses. Next, the thermal

* Corresponding author at: CAS Key Laboratory of Soft Matter Chemistry, Department of Chemistry, University of Science and Technology of China, Hefei 230026, PR China.
E-mail address: solexin@ustc.edu.cn (L.X. Song).

0040-6031/$ – see front matter © 2010 Elsevier B.V. All rights reserved.
doi:10.1016/j.tca.2010.04.031

Table 1
Positions of main peaks from left to right in TIC profiles of α-, β-, γ-, DMβ-, HPβ- and PAA–β-CD.

Samples	Heating time (t/min)						Corresponding temperature (T/K)						Refs
	t_1	t_2	t_3	t_4	t_5	t_6	T_1	T_2	T_3	T_4	T_5	T_6	
α-CD	–	19.47 (s)[a]	25.30 (w)	28.00 (w)	31.67 (w)	–	–	553	647	653	773	–	[24]
β-CD	–	–	25.63 (s)	27.23 (m)	–	–	–	–	653	653	–	–	[23]
γ-CD	–	20.19 (s)	25.07 (s)	–	31.67 (w)	–	–	553	629	–	773	–	–
DMβ-CD	10.65 (w)	20.72 (m, b)	25.34 (s)	–	31.82 (w)	35.76 (w)	463	553	650	–	773	773	–
HPβ-CD	–	–	25.69 (s)	27.58 (s)	32.12 (w)	36.74 (w)	–	–	653	653	773	773	–

[a] Alphabets s, m, w and b represent strong, moderate, weak and broad peaks.

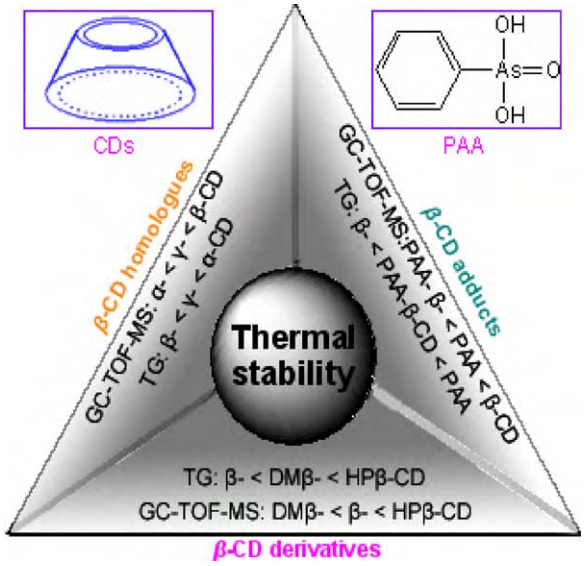

Fig. 1. Comparison of the thermal stabilities of α-, β-, γ-, HPβ-, DMβ-CD, PAA and PAA–β-CD.

degradation mechanisms of β-CD and its two derivatives: mono(2-*O*-2-hydroxypropyl)-β- (HPβ-) and heptakis(2,6-di-*O*-methyl)-β- (DMβ-CD) are investigated and compared carefully. And then, we explore the formation of the adduct of β-CD with PAA in solution and evaluate the difference in thermal behaviors of two solid adducts, SA–β-CD [24] and PAA–β-CD. Finally, the results from Fourier transformation infrared (FTIR) spectroscopy, powder X-ray diffraction (PXRD) and field emission scanning electron microscopy (FESEM) are used to explain and interpret the variation observed in thermal degradation behaviors of homologues, derivatives and adducts of β-CD.

Our results on the thermal stabilities of α-, β-, γ-, HPβ-, DMβ-CD, PAA and PAA–β-CD under TG and GC–TOF-MS conditions (see Fig. 1) provide new and important information about how macrocyclic conformations, chemical modifications and simple adduct behaviors of the carbohydrates dramatically affect their thermal stability.

2. Experimental

2.1. Materials

α- and β-CD were purchased from Nihon Toshin Chemical Company and Shanghai Chemical Reagent Company, respectively. DMβ- and γ-CD were kindly donated by Harata. HPβ-CD was purchased from Shandong Xinda Fine Chemical Company. PAA was purchased from Shanghai Joint State-Private Liberal Chemical Company. All other chemicals were of general-purpose reagent grade unless otherwise stated. All samples were kept under the same conditions, *i.e.*, stored in a vacuum drier under 323 K for 24 h before use.

2.2. Preparation of solid adduct of β-CD with PAA

The solid adduct PAA–β-CD was prepared by mixing PAA (101 mg, 0.5 mmol) and β-CD (567 mg, 0.5 mmol) in 100 ml of deionized water and stirring for 2 h at 333 K. Then solvent was drawn off by rotary evaporation under vacuum at 323 K. A white powdery product was obtained in 98% yield (655 mg), and kept in a desiccator.

2.3. Adduct interaction of CDs with PAA in water

The stock solutions of CDs and PAA were freshly prepared by dissolving solid samples in deionized water. The concentration of PAA was kept constant at 5.00×10^{-5} mol dm^{-3}, while the concentrations of α-, β-, γ-, HPβ- and DMβ-CD varied from 0.00 to 4.00×10^{-3} mol dm^{-3}. The solutions of PAA and CDs were mixed in a beaker at 298 K with stirring for 20 min. And then, the mixed solution was measured using a UV–vis spectrophotometer.

2.4. Instruments and methods

PXRD patterns of samples were recorded in a Philips X'Pert Pro X-ray diffractometer. All the samples were irradiated with monochromatized Cu Kα and analyzed with $0^\circ \leq 2\theta \leq 40^\circ$. Tube voltage and current were 40 kV and 40 mA, respectively. FTIR spectra were made on a Bruker Equinox 55 spectrometer in KBr pellets in the 4000–400 cm^{-1} range. FESEM images of samples were recorded on a JEOL-JSM-6700F field-emitting microscope. UV–vis spectra were recorded on a Shimadzu UV 2401-(PC) spectrometer in the range 190–350 nm. TG and DTG analyses were performed on a Shimadzu TGA-50 thermogravimetric analyzer at a constant heating rate of 10 K min^{-1} under a nitrogen atmosphere with a gas flow of 25 ml min^{-1}. GC–TOF-MS measurements with a programmed temperature operation were carried out with a Micromass GCT-MS spectrometer using a direct insertion probe for solid samples at the same heating program as reported previously [23].

3. Results and discussion

3.1. Differences in thermal degradation pathways of β-CD and its two homologues

Many studies indicated that the mass losses of α-, β- and γ-CD in TG curves can be roughly divided into four stages in light of temperature range: a dehydration process from 298 to 390 K, a long plateau region from 390 to 572 K, a rapid decomposition from 572 to 626 K and a carbonization or incineration process from 626 to 875 K [10,25–28]. Except that there are some differences at the dehydration stage, the three parent CDs exhibit rather similar TG characteristics [25,29–31]. However, the present work based on GC–TOF-MS analyses sufficiently expresses unexpected differences in thermal behaviors among them.

Table 1 summarizes the relationship between the position of main peaks and heating times in total ion current (TIC) curves of α-, β- and γ-CD under the same conditions. In the early time windows, γ-CD shows a similar thermal behavior as α-CD since they both start to abruptly decompose at relatively lower temperatures, *i.e.*, 553 K. Later, no strong signals are observed in the TIC curve of α-CD, indicating there is only one release process which is responsible for its main decomposition. This is significantly different from the cases of β- and γ-CD, in which there are two major decomposition signals. But then there is a large difference in position between β- and γ-CD, as shown in Table 1.

The comparison of positions of main peaks in the TIC curves gives a strong impression that the thermal stabilities of the three parent CDs increase in the order α- < γ- < β-CD in vacuum.

Fig. 2 reports mass spectra of substances emitted from α-, β- and γ-CD at 553 K. At this temperature, there are similarity and difference of decomposition routes of the three CDs. The decomposition of α-CD produces three main fragments: m/z 57.034 ($CH_2CH_2CHO^+$), 60.020 ($C_2H_4O_2^+$) and 73.029 ($C_3H_5O_2^+$), corresponding to the cleavage of one or more of C–O and C–C bonds in glucopyranose units [24].

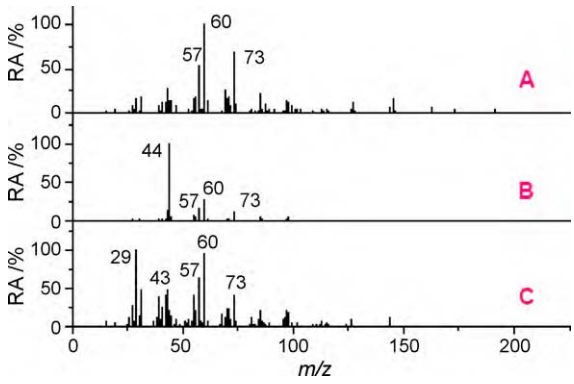

Fig. 2. Mass spectra of decomposition products of α- (A), β- (B) and γ-CD (C) at 553 K.

Table 2
FTIR data of α-, β-, γ-, DMβ-, HPβ- and PAA–β-CD.

Samples	Main vibration bands/cm^{-1}			
	υ_{O-H}	δ_{O-H}	υ_{C-H}	υ_{C-O}
α-CD	3413	1641	2926	1032
β-CD	3424	1637	2923	1030
γ-CD	3414	1639	2930	1027
DMβ-CD	3446	1632	2934	1042
HPβ-CD	3425	1634	2928	1038
PAA–β-CD	3393	1637	2928	1029

γ-CD has a similar decomposition characteristic with α-CD, except the occurrence of the small fragments: m/z 29.002 (CHO^+) and 43.020 (CH_2CHO^+) in high relative abundances (RA, %). The structural transformation from $CH_2CH_2CHO^+$, CH_2CHO^+ to CHO^+ indicates that the glucopyranose units in γ-CD are degraded more efficiently than in α-CD. However, in the case of β-CD, all these signals become quite weak. Instead, the strongest signal occurs at m/z 43.990 (CO_2^+). This implies that the rupture of 1,4-glycosidic bonds is the most important degradation pathway of β-CD at this time [32].

The large difference in decomposition behavior of β-CD and its two homologues can be reflected by structural differences of them, such as hydrogen bonding networks: υ_{O-H}, 3413 (α-), 3424 (β-) and 3414 cm^{-1} (γ-CD, see Table 2), positions of 2θ angles at the first (I_1), second (I_2) and third (I_3) strongest peaks in molecular stacking forms: 11.9, 14.3 and 21.6° (α-), 12.6, 17.3 and 22.9° (β-), and 10.2, 20.4 and 18.7° (γ-CD, see Table 3) [31], crystal surface properties, especially their macrocyclic conformations [33].

Fig. 3 displays that α-, β- and γ-CD are in the shape of a long strip, a hexagonal prism and a blocky structure, respectively. Structural data reported in the literature showed that the macrocyclic conformation of the CDs is in relation to the number of glucose units [34]. In short, β-CD not only has a different macrocyclic structure from α- and γ-CD, but also exhibits the best morphology under the same

Table 3
Positions of I_1, I_2 and I_3 in PXRD patterns of α-, β-, γ-, DMβ-, HPβ-, PAA–β-CD and PAA.

Samples	2θ angles/°		
	I_1	I_2	I_3
α-CD	11.9 (s)	14.3 (s)	21.6 (s)
β-CD	12.6 (s)	17.3 (m, s)	22.9 (m, s)
γ-CD	10.2 (s)	20.4 (m, s)	18.7 (m, s)
DMβ-CD	10.6 (w, b)	18.9 (w, b)	–
HPβ-CD	19.3 (m, b)	10.1 (w, b)	–
PAA–β-CD	19.0 (s)	17.9 (m, s)	12.5 (m, s)
PAA	18.0 (s)	10.6 (s)	24.9 (s)

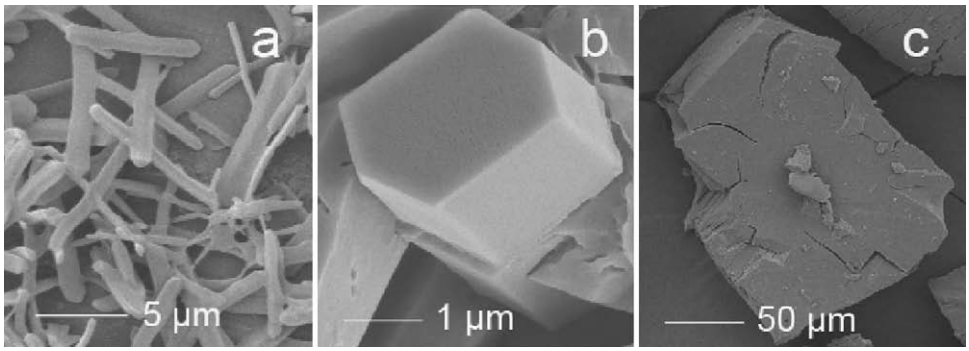

Fig. 3. FESEM images of α- (a), β- (b) and γ-CD (c).

crystallization condition. These may be important reasons for the fact that the decomposition pathway of β-CD differs from the other two.

3.2. Differences in thermal behaviors of β-CD and its two derivatives

The TG curves of β-, DMβ- and HPβ-CD are shown in Fig. 4. Obviously, the decomposition temperature points of DMβ- and HPβ-CD are much higher than that of β-CD during the whole rapid decomposition processes. For example, when the residual mass (RM, %) of samples is 50%, the decomposition temperature difference (ΔT/K) between β-CD and its derivates is higher than 30 K. In a word, the thermal stabilities of DMβ- and HPβ-CD are enhanced due to the modification. Such results can also be directly drawn from the temperatures of maximum decomposition rate: 592 (β-), 629 (DMβ-) and 638 K (HPβ-) in DTG profiles [31].

In addition, the temperatures of the swift decomposition end are different: 626 (β-), 646 (DMβ-) and 660 K (HPβ-CD). After that, the RM value of β-CD is always higher than those of DMβ- and HPβ-CD. For instance, at the end temperature (873 K), the RM values of β-, DMβ- and HPβ-CD are 8.96, 2.31 and 1.80%, respectively. The result indicates that the two derivatives decompose far more completely than β-CD. This may be associated with the fact that DMβ- and HPβ-CD have a loose structure with loose stitches that can be established by crystal behaviors, since PXRD patterns of them, unlike β-CD, only exhibit two broad peaks at 10.6 and 18.9°, and 10.1 and 19.3°, respectively [31]. This indicates that the chemical modification of hydroxyl groups leads to poor crystallization.

From the FTIR data in Table 2, the stretching vibration bands of O–H, C–O and C–H of the two derivatives all shift to higher wavenumbers when compared to those of β-CD. The blue shift of the O–H band means that hydrogen bond interactions in these molecules are affected after modification. The difference in change of the O–H bonds of the two CDs can be explained by different electron-donating effects of fourteen methyl groups and one hydroxypropyl group. Maybe the variation of hydrogen bonding networks is one reason why they have a better thermal stability than β-CD.

Also, the two derivatives show a highly similar decomposition property since the stage of rapid decomposition of them almost occurs simultaneously. TG profiles do not provide insights into the decomposition processes involved. How do we explain the similarity between them and the difference between β-CD and them? Therefore, GC–TOF-MS measurements are employed to provide detailed information concerning the correlation between distributions of cleaved fragments and positions of substituent groups.

TIC data of DMβ- and HPβ-CD show that although there are only two strong signals in the curves, their positions, shapes and intensities are rather different from each other, as shown in Fig. 5. Clearly, the thermal decomposition of HPβ-CD is slightly delayed while that of DMβ-CD is obviously advanced relative to β-CD under the same GC–TOF-MS conditions. This result not only forcefully demonstrates the influence of substituent groups on the thermal degradation of β-CD, but also adequately reveals these carbohydrates have different thermal behaviors under different atmospheres (nitrogen in TG and vacuum in GC–TOF-MS).

The effect of substituent groups on ruptures of C–O and C–C bonds in glucopyranose units is seen from the comparison of mass spectra (see Figs. 2B and 6) of β-CD and its derivatives at the same heating time. The two derivatives show different decomposition patterns from β-CD at 553 K. For instance, some of HPβ-CD molecules decompose into two major fragments: m/z

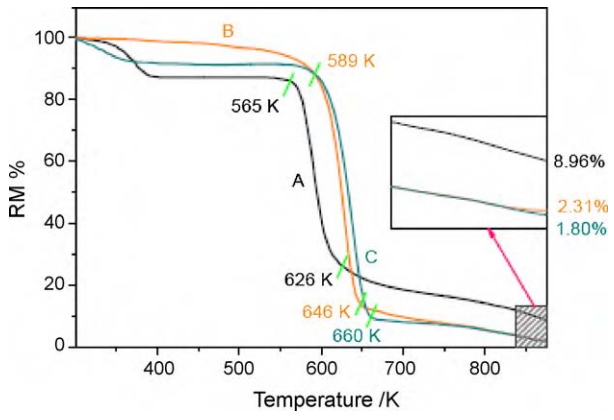

Fig. 4. TG profiles of β- (A), DMβ- (B) and HPβ-CD (C) at the heating rate of 10 K min^{-1}.

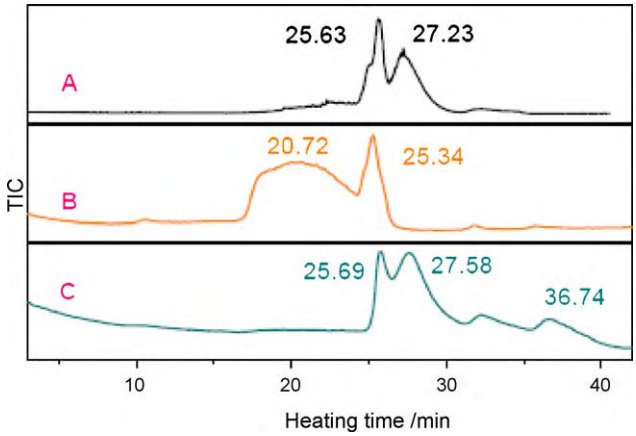

Fig. 5. TIC curves of free β-CD (A), DMβ-CD (B) and HPβ-CD (C).

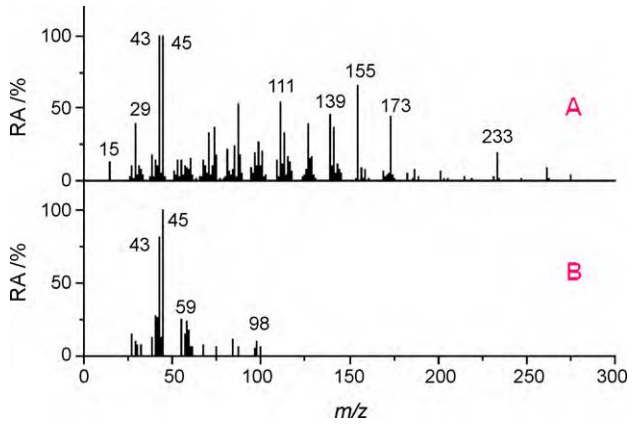

Fig. 6. Mass spectra of decomposition products of DMβ- (A) and HPβ-CD (B) at 553 K.

43.020 ($C_2H_3O^+$, 81.80%) and 45.034 ($C_2H_5O^+$, 100.0%). At this temperature, DMβ-CD gives more main fragments such as m/z 43.020 (100.0%), 45.034 (98.90%), 155.071 ($C_8H_{11}O_3^+$, 65.18%) and so on.

Interestingly, the formation of many fragment signals from HPβ-, DMβ-CD, such as m/z 15.023 (CH_3^+), 45.034 ($C_2H_5O^+$) and 59.050 ($C_3H_7O^+$) are associated with introduced sites of the groups: hydroxypropyl group and methyl group (see Fig. 7). Their RA values increase with the increase of temperature. Some of these fragments appear and show high RA values even at lower temperatures such as 463 K, indicating that the introduced groups are easy to break off when heating. The fragment at m/z 155.071 comes from the degradation of a modified glucose unit, as shown in Fig. 7.

The fact that this fragment has a high RA value gives a hint that the unmodified C-3 hydroxyl group in DMβ-CD is sensitive to heating, which serves possibly the purpose of selective modification in organic synthesis. Also, from an academic as well as a technological point of view, it is very interesting and important to point out the structural change from a glucopyranose polymer to a heterocyclic compound.

The phenomena described above suggest that we should be very careful when using β-CD derivatives to improve the absorption, solubility and separation of drugs. For example, when β-CD derivatives are used as stationary-phase components in gas chromatography as well as mobile-phase additives in liquid chromatography [35,36], the effect of the temperature of chromatographic columns

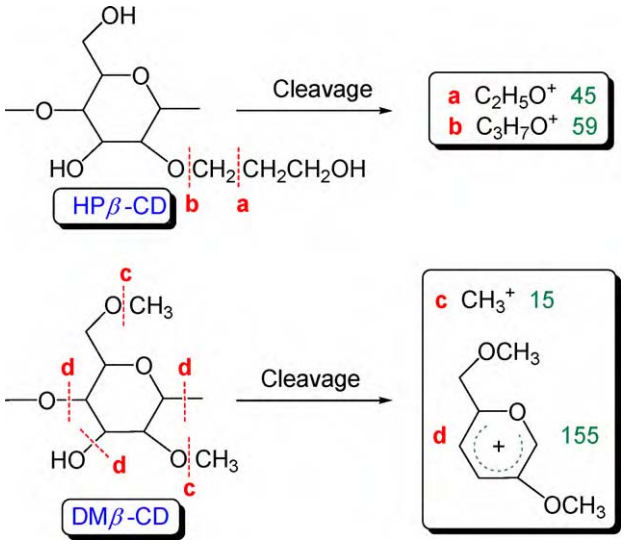

Fig. 7. Proposed rupture models of HPβ- and DMβ-CD at 553 K.

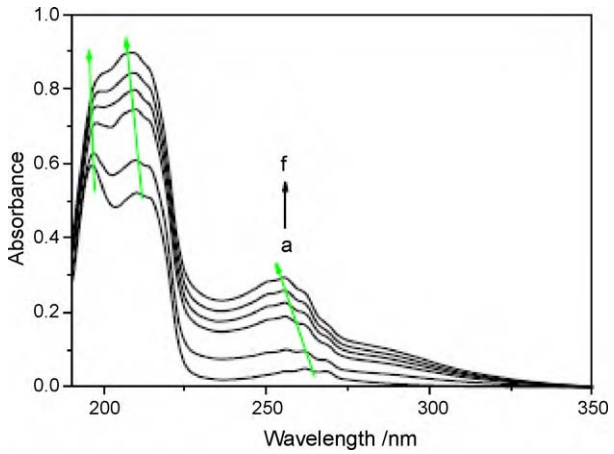

Fig. 8. UV–vis spectra of PAA (5.00×10^{-5} mol dm^{-3}) in the absence and presence of DMβ-CD. The concentrations of DMβ-CD from a to f are 0.00, 2.00, 2.50, 3.00, 3.50, 4.00×10^{-3} mol dm^{-3}.

on the thermal release of the substituent groups needs to be considered.

3.3. Differences in thermal behaviors of β-CD and its adduct

3.3.1. No observable adduct phenomenon between β-CD and PAA in solution

The absorbance of free PAA at 268 nm is due to the presence of benzene ring, and two moderate peaks at 196 and 210 nm are caused by As–O and As=O bonds absorption. As shown in Fig. 8, the intensity of the absorption bands increases and the bands exhibit a slight blue shift with increasing concentration of DMβ-CD. This phenomenon is also observed in PAA–α-CD and PAA–HPβ-CD systems, but does not appear in PAA–β-CD and PAA–γ-CD systems. The results show that the CDs themselves have no absorption in the wavelength range from 190 to 350 nm, and there are no changes of pH and ionic strength before and after mixing the solutions. Hence, these changes in UV–vis spectra imply that a large change occurs in chemical environment of PAA, which can be explained by the transference of PAA from water to hydrophobic cavity of α-, DMβ- or HPβ-CD.

Such a large difference in adduct behaviors between β-CD and its derivatives leads us to ask if an observable adduct phenomenon of two components in solution is a necessary condition for the formation of a solid adduct of the two components.

3.3.2. Thermal behavior comparison of β-CD and its solid adduct of PAA

The relationship between heating temperatures and decomposition behaviors of β-CD, PAA and their adduct PAA–β-CD under nitrogen atmosphere, is drawn in Fig. 9. The profiles of the curves in the figure provide important information. Thermal decomposition of PAA occurs much earlier (from 663 to 603 K) after adduct, but the main decomposition stage of β-CD is slightly delayed (from 590 to 603 K), and that the adduct is decomposed more completely than both PAA and β-CD at higher than 800 K. The big difference between the TG/DTG curve of the adduct and the fitted theoretical curve based on a mixed form of β-CD and PAA in a 1:1 molar ratio reveals there is an interaction between β-CD and PAA.

This observation is demonstrated by the data presented in Tables 2 and 3. On one hand, the υ_{O-H} vibration band of β-CD has shifted to a lower wavenumber from 3424 to 3393 cm^{-1} upon adduct, suggesting a big difference of hydrogen bonding interaction between β-CD molecules from free state to the adduct state. On the other hand, it is shown that some new peaks appear in the

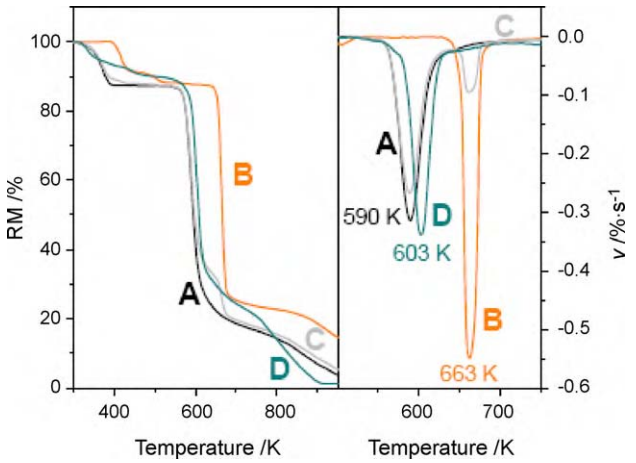

Fig. 9. TG and DTG profiles of β-CD (A), PAA (B), the fitted theoretical curve based on a mixed form of β-CD and PAA in a 1:1 molar ratio (C) and PAA–β-CD adduct (D) at the heating rate of 10 K min^{-1}.

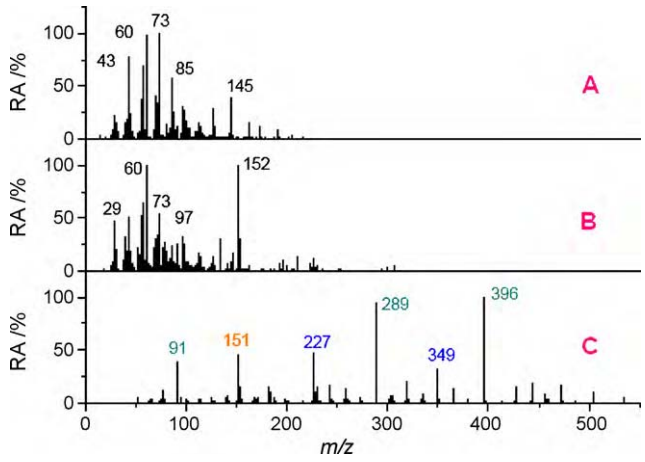

Fig. 11. Mass spectra of decomposition products of β-CD (A), PAA (B) and PAA–β-CD (C) at 25.41 min.

PXRD pattern of PAA–β-CD, which are not observed in those of PAA and β-CD [31].

GC–TOF-MS measurements further confirm the existence of the intermolecular interaction between them. Fig. 10 describes the TIC curves of PAA and its adduct. Surprisingly, the adduct has an extra new peak at 10.09 min, which is found neither in free β-CD nor in PAA. Data from the mass spectrum at this moment indicate the thermal release is mainly involved in the decomposition of PAA [31]. Consequently, the occurrence of the new peak with moderate intensity means that the interaction between β-CD and PAA results in a decrease in thermal stability of PAA. This is in good accordance with TG/DTG analysis.

A series of mass spectra at different heating times are analyzed and compared in order to further investigate how the adduct interaction between the two components affects their thermal release behaviors in different decomposition stages. Fig. 11 shows the mass spectra of decomposition products of β-CD, PAA and PAA–β-CD at 25.41 min (653 K). The main decomposition processes of these samples start at the moment approximately corresponding to the maximum peak in their TIC curves. The strong peaks at m/z 29.002 (CHO^+, 47.64%), 57.034 ($C_3H_5O^+$, 63.62%), 60.020 ($C_2H_4O_2{}^+$, 98.97%) and 73.029 ($C_3H_5O_2{}^+$, 53.21%) in the mass spectrum of free PAA are attributable to the breakdown of the benzene ring and the recombination among fragments. The strongest signal at m/z 151.961 is due to the release of the $C_6H_5As^+$ ion. At this temperature, free β-CD decomposes and produces many small molecular ions, such as $C_2H_3O^+$, $C_2H_4O_2{}^+$ and $C_3H_5O_2{}^+$ ions.

However, there is an unexpected result in the figure, namely, that in the case of the adduct, this spectrum is mainly represented by a series of peaks of inorganic arsenic oxides, such as 90.917 (AsO^+, 37.94%), 288.744 ($As_3O_4{}^+$, 93.93%) and 395.654 ($As_4O_6{}^+$, 100.0%), as well as some large organic arsenic compounds, such as 226.985 ($C_{12}H_8As^+$, 47.31%) and 348.778 ($C_6H_4O_3As_3{}^+$, 32.45%). Possibly, the presence of β-CD leads to the ionization of the $C_6H_5As^+$ ion resulted from the decomposition of PAA, producing $C_6H_4As^+$ ion (150.954, 45.94%). Proposed formation processes of the two ions are illustrated in Fig. 12. The fact that all important fragment signals in the spectrum of the adduct are associated with arsenic compounds suggests that the degradation mechanisms of PAA and β-CD after adduct have changed thoroughly.

Fig. 13 displays the mass spectra of decomposition products of β-CD, PAA and PAA–β-CD at 31.72 min (773 K). These signals in the spectra directly reflect the information on the final decomposition processes of PAA and its adduct (see Fig. 13). At this stage, free β-CD only releases a few fragments of $CO_2{}^+$ ions, and the liberation of free PAA was mainly in the form of simple substances of arsenic, such as As^+ (74.923, 40.60%), $As_2{}^+$ (149.844, 40.77%) $As_3{}^+$ (224.765, 19.81%) and $As_4{}^+$ (299.685, 100.0%). The RA values of the simple substances of arsenic are approximately in agreement with their stabilities: $As_4{}^+ > As_2{}^+ > As^+ > As_3{}^+$ [24].

A difference between Figs. 11A and 13A, as well as Figs. 11B and 13B, and a similarity between Figs. 11C and 13C sufficiently demonstrate the effect of adduct interaction on the decomposition mechanisms of the adducted components. The phenomenon that at the end stage no observable signals of these arsenic forms occur in the spectrum of the adduct differs from that encountered in the case of the adduct of $NaAsO_2$ and β-CD [24]. This reveals different effects of adduct interactions on thermal behaviors of organic arsenic and inorganic arsenic compounds.

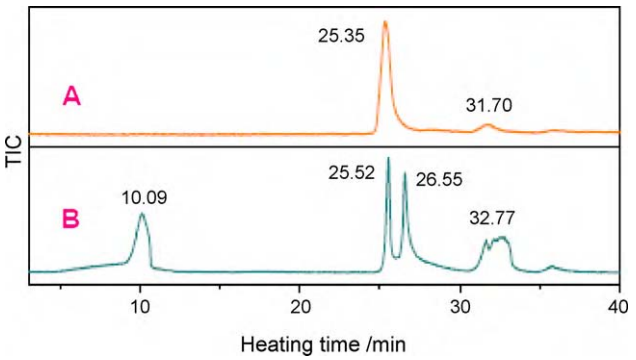

Fig. 10. TIC curves of PAA (A) and PAA–β-CD (B).

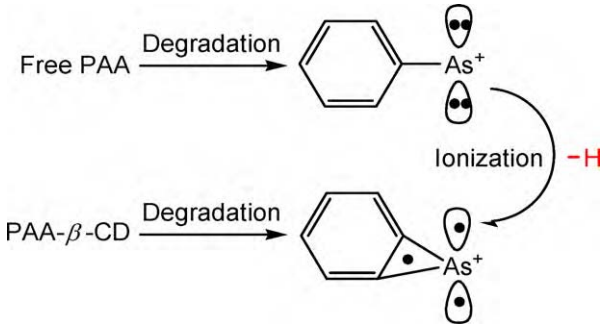

Fig. 12. Proposed formation process of $C_6H_5As^+$ and $C_6H_4As^+$ ions from PAA and PAA–β-CD, respectively.

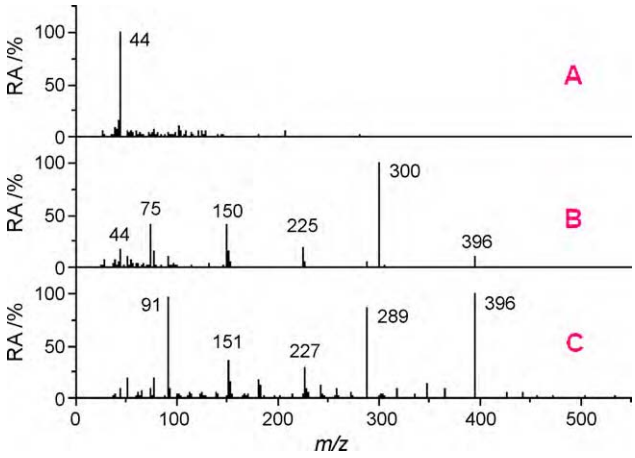

Fig. 13. Mass spectra of decomposition products of β-CD (A), PAA (B) and PAA–β-CD (C) at 31.72 min.

The information provided does give an implication that when β-CD is applied to the encapsulation of organic and inorganic drugs in molecular level, we have to take into consideration the possible effects of adduct interaction between them so as to prevent the formation of toxic intermediates during heating.

4. Conclusions

The studies presented in this paper focus on the differences in thermal degradation behaviors of homologues (α- and γ-), derivatives (DMβ- and HPβ-CD) and adducts (PAA–β-CD and $NaAsO_2$–β-CD) of β-CD. The results reveal several important findings. First, different macrocyclic conformations cause different decomposition mechanisms of β-CD and its two homologues, inducing different thermal stabilities among them. Second, the introduction of substituent groups has enhanced the thermal performance of β-CD to a different extent, and the contrast sensitivity of introduced groups to heating fields gives an alert for possible practical application of CD derivatives. Third, although the adduct interaction between β-CD and PAA is not observed by UV–vis spectroscopy in solution, the prepared adduct PAA–β-CD shows a distinctive characteristic of thermal decomposition from PAA, β-CD and $NaAsO_2$–β-CD. Finally, our results indicate different atmospheres result in different orders in the stabilities of the carbohydrates. Such interesting results offer significant insights into application of chemical modification and molecular encapsulation of carbohydrates.

Acknowledgements

We acknowledge the funding support received for this research project from Natural Science Foundation of Anhui Province (No. 090416228).

Appendix A. Supplementary data

Supplementary data associated with this article can be found, in the online version, at doi:10.1016/j.tca.2010.04.031.

References

[1] A. Harada, M. Osaki, Y. Takashima, H. Yamaguchi, Acc. Chem. Res. 41 (2008) 1143–1152.
[2] L.X. Song, L. Bai, X.M. Xu, J. He, S.Z. Pan, Coord. Chem. Rev. 253 (2009) 1276–1284.
[3] Y. Yu, W.S. Cai, C. Chipot, T.T. Sun, X.G. Shao, J. Phys. Chem. B 112 (2008) 5268–5271.
[4] L.X. Song, L. Bai, J. Phys. Chem. B 113 (2009) 11724–11731.
[5] A. Harada, Acc. Chem. Res. 34 (2001) 456–464.
[6] W.S. Cai, T.T. Sun, P. Liu, C. Chipot, X.G. Shao, J. Phys. Chem. B 113 (2009) 7836–7843.
[7] B. Barkakaty, K. Matsumoto, T. Endo, Macromolecules 42 (2009) 9481–9485.
[8] L.X. Song, H.M. Wang, X.Q. Guo, L. Bai, J. Org. Chem. 73 (2008) 8305–8316.
[9] L.P. Fernandes, W.P. Oliveira, J. Sztatisz, I.M. Szilagyi, C. Novak, J. Therm. Anal. Cal. 95 (2009) 855–863.
[10] Z. Ehen, F. Giordano, J. Sztatisz, L. Jicsinszky, C. Novak, J. Therm. Anal. Cal. 80 (2005) 419–424.
[11] Y. Liu, R. Cao, Y. Chen, J.Y. He, J. Phys. Chem. B 112 (2008) 1445–1450.
[12] L. Szente, J. Szejtli, Adv. Drug Deliv. Rev. 36 (1999) 17–28.
[13] K. Uekama, F. Hirayama, T. Irie, Chem. Rev. 98 (1998) 2045–2076.
[14] F. Maestrelli, M. Cecchi, M. Cirri, G. Capasso, N. Mennini, P. Mura, J. Incl. Phenom. Macrocycl. Chem. 63 (2009) 17–25.
[15] T. Kraus, M. Budesinsky, J. Zavada, J. Org. Chem. 13 (2001) 4595–4600.
[16] B.Y. Yu, J.W. Chung, S.Y. Kwak, Environ. Sci. Technol. 42 (2008) 7522–7527.
[17] A. Perl, L. Kumprecht, T. Kraus, D. Armspach, D. Matt, D.N. Reinhoudt, J. Huskens, Langmuir 25 (2009) 1534–1539.
[18] B.E. Ragle, V.A. Karginov, J.B. Wardenburg, Antimicrob. Agents Chemother. 54 (2010) 298–304.
[19] L. Kumprecht, M. Budesinsky, J. Vondrasek, J. Vymetal, J. Cerny, I. Cisarova, J. Brynda, V. Herzig, P. Koutnik, J. Zavada, T. Kraus, J. Org. Chem. 74 (2009) 1082–1092.
[20] M. Hasegawa, S. Yamamoto, M. Kobayashi, H. Kise, Enzyme Microb. Technol. 32 (2003) 356–361.
[21] A.D. Martins, A.A. Craveiro, M.I.L. Machado, F.N. Raffin, T.F. Moura, C. Novak, Z. Ehen, J. Therm. Anal. Cal. 88 (2007) 363–371.
[22] G. Lazzara, S. Milioto, J. Phys. Chem. B 112 (2008) 11887–11895.
[23] L.X. Song, X. Peng, J. Phys. Chem. A 112 (2008) 11341–11348.
[24] L.X. Song, Z. Dang, J. Phys. Chem. B 113 (2009) 4998–5000.
[25] F. Giordano, C. Novak, J.R. Moyano, Thermochim. Acta 380 (2001) 123–151.
[26] L.X. Song, H.M. Wang, Y. Yang, P. Xu, Bull. Chem. Soc. Jpn. 80 (2007) 2185–2195.
[27] D. Plackett, A. Ghanbari-Siahkali, L. Szente, J. Appl. Polym. Sci. 105 (2007) 2850–2857.
[28] F. Trotta, M. Zanetti, G. Camino, Polym. Degrad. Stab. 69 (2000) 373–379.
[29] V. Berbenni, A. Marini, G. Bruni, Thermochim. Acta 322 (1998) 137–151.
[30] A. Marini, M. Villa, V. Berbenni, G. Bruni, V. Massarotti, P. Mustarelli, J. Chem. Phys. 103 (1995) 7532–7540.
[31] See the Supporting Information.
[32] P. Xu, L.X. Song, H.M. Wang, Thermochim. Acta 469 (2008) 36–42.
[33] K. Harata, Chem. Rev. 98 (1998) 1803–1827.
[34] J. Szejtli, in: J. Szejtli, T. Osa (Eds.), Comprehensive Supramolecular Chemistry (CDs), Pergamon, Oxford, 1996.
[35] P.K. Zarzycki, E. Wlodarczyk, M.J. Baran, J. Chromatogr. A 1216 (2009) 7602–7611.
[36] A. Rocco, S. Fanali, J. Sep. Sci. 32 (2009) 1696–1703.